Evaluations of Flow and Mixing Efficiency in the Kneading Disks of a Novel Tri-Screw Extruder

X. Z. Zhu[†], T. S. Wang and G. Wang

School of Mechanical Engineering, Liaoning Shihua University, Fushun Liaoning 113001, China

†*Corresponding Author Email: xzzhu@126.com*

ABSTRACT

The forward or backward stagger angles of the kneading disks have great effects on configures of the special center region along axial length in a novel tri-screw extruder. In this paper, the flow and mixing of a non-Newtonian polyethylene in kneading disks of a tri-screw extruder were simulated using three-dimensional finite element modeling based on mesh superposition technique. Three types of kneading disks, neutral stagger, staggered 30° forward and staggered 30° reverse were considered for the tri-screw extruder. The effects of stagger angles of kneading disks on the flow pattern in the tri-screw extruder were investigated. Moreover, at different stagger angles, the dispersive and distributive mixing efficiencies in the kneading disks of the tri-screw extruder and the twin-screw extruder were calculated and compared by means of mean shear rate, stretching rates, maximal stress magnitudes, mixing index, residence time distribution (RTD) and logarithm of area stretch. It is found that increasing the stagger angles decreases the axial velocities of polymer melt in the center region for the tri-screw extruder. The staggered 30° reverse is relatively reasonable for the tri-screw extruder and neutral stagger for the twin-screw extruder for the mixing efficiency. In comparison, the kneading disks in the tri-screw extruder have higher distributive and dispersive mixing efficiencies than those in the twin-screw extruder with the same stagger angles.

Keywords: Kneading disks of tri-screw extruders; Stagger angles; Mixing efficiency; Residence time distribution; Finite element method.

NOMENCLATURE

a	width of the transition region between η_0 and n.	**W**	norm of the vorticity tensor
$c(t)$	concentration of the trajectories at the exit		
D	rate of deformation tensor	τ	stress tensor
da	surface deformation at time	η	shear viscosity
d**A**	an infinitesimal surface	$\dot{\gamma}$	effective shear rate
$E(t)$	density function of residence time	η_∞	infinite shear viscosity
$F(t)$	accumulative residence time distribution function	η_0	viscosity at zero shear viscosity
n	the power-law index	λ	model-specific relaxation time
P	fluid pressure	II_D	second invariant of deformation tensor rate
T_0	smallest time observed in the exit plane	Δt	iterative time step
T_{75}	75% of the particles flow out of the exit	ΔT	mean $T_{75} - T_0$
V	velocity vector distribution	λ_{MZ}	mixing index
		η	area of stretch

1. INTRODUCTIONS

Twin-screw extruders are a very common type of extruders in polymer processing. Recently, with the development of polymer industry, especially for the nanocomposite processing, a novel tri-screw extruder is explored due to its strong shear force and higher mixing efficiency (Huang and Chen, 2009; Jiang and Zhu, 2001). The tri-screw extruder has one more screw than the twin-screw extruder. Also, it has three intermeshing regions and one dynamic center region. Therefore, as a complex mixing setup for polymer processing, the modeling and computational simulation of the tri-screw

extruder remain very challenging, especially for the special dynamic center region with period changes of areas and geometric shapes (Zhu *et al.*, 2009).

A complete modular screw in the tri-screw extruder mainly consists of conveying, melt, mixing, pressurizing, and pump sections. The compound may include a polymer or a polymer blend and a number of additives. Thus, the mixing section is an important step, which evidently affects the quality of final product. So far, the studies on the flow and mixing profiles in the tri-screw extruders mainly focus on the convey elements. While conventional screws do not provide high mixing efficiency. Not much published work is available on the analysis of the effects of stagger angles on the flow and mixing in the mixing sections of tri-screw extruders.

In previous researches, Jiang and Zhu (2008) employed the simulation and experiments to verify the stronger conveying capacity in the tri-screw extruder. The high shear frequency of material in the tri-screw extruder was also found. Hu *et al.* (2004, 2006) studied the mean mixing characteristics of the tri-screw and twin-screw extruders using the finite element analysis codes, Polyflow. Based on the calculated velocity fields, the particle trajectories in both machines were visualized using particle tracking technique. Zhu *et al.* (2009) established a quasi-three-dimensional modeling to simulate polymer melts flowing in a convey element of the tri-screw extruders with FEM. The temperature distributions, energy consumption and capacity ratio in a tri-screw extruder at different screw geometric parameters and operational conditions were studied. More recently, Wang *et al.* (2013) established a 2D modeling to study the effects of screw clearances on the mixing mechanism of tri-screw extruders. The mixing evaluations and mechanics characteristics of tri-screw extruder were studied with different screw clearances and compared with twin screw extruder. Zhu *et al.* (2013a) investigated the effects of dynamic center region on the flow and mixing efficiency of a convey element in a tri-screw extruder using 3D finite element modeling. The special contributions of the center region to the entire convey section in tri-screw extruders of axial flow and mixing efficiency were discussed. In particular, the nonlinear dynamics of typical particle motions in the center region and the mixing process in the tri-screw extruder were analyzed with Fast Fourier transform (FFT) spectrums and Poincaré maps using a 2D finite element modeling to study the effect of the dynamic motions in the center region (Zhu *et al.*, 2013b). However, no much flow and mixing information in the kneading disks of tri-screw extruders was presented with considering the effects of stagger angles.

With the recent advances in computational fluid dynamics to solve the problems related to rotational fluid mechanics ( ), a large number of studies on the flow and mixing mechanism in the kneading disks of the twin-screw extruders use finite element method (FEM) and finite volume method (FVM) (For example, Alsteens *et al.*,2004; Bravo *et al.*, 2004; Ishikawa *et al.*, 2001; Ghoreishy *et al.*, 2005;

Nakayama *et al.*, 2011; Rafei *et al.*, 2009; Sobhani *et al.*, 2010; Yoshinaga *et al.*, 2000; Zhang *et al.*,2009.). In a way, although similar in structure and design to the twin-screw extruder, the tri-screw extruder is different from the twin-screw extruder in the flow and mixing mechanisms. From previous researches, it is known that most of particles initial distribution in the inlet plane of the center region fast flow out the outlet and don't pass through any screw in convey element of the tri-screw extruder (Hu *et al.*, 2006; Zhu *et al.* 2013). This special phenomenon may be changed in the kneading disks with the forward or backward stagger angles for the tri-screw extruder. This is due to the fact that the stagger angle has great effect on configures of the center region along axial length in the tri-screw extruder. Therefore, the effects of stagger angles on flow and mixing mechanisms in the kneading disks of the tri-screw extruder are different from the traditional twin-screw extruder and should be pay more attention to understand the special flow and mixing efficiency to enhance their optimization design with great practical significance.

In this work, three-dimensional finite element modeling of polymer melt flow and mixing in the kneading disks of a novel tri-screw extruder was established with mesh superposition technique. The flow visualizations in the kneading disks of tri-screw extruders were carried out with particle trajectories. The effects of stagger angles of kneading disks on the flow patterns in the tri-screw extruder were investigated. Moreover, the dispersive and distributive mixing efficiencies in the kneading disks of the tri-screw extruder and the twin-screw extruder were calculated and compared by means of the mean shear rate, stretching rates, maximal stress magnitudes, mixing index, residence time distribution (RTD) and logarithm of the area stretch, respectively. The main objective is to better understand the special flow and mixing mechanisms in the kneading disks of tri-screw extruders, especially for the effects of stagger angles on the flow and mixing efficiency in the kneading disks. It is help to enhance the optimization design of tri-screw extruders.

2. METHODS AND MATERIALS

2.1 Mathematical Modeling

In this work, the 3D time-dependent flow conditions are considered. The flow domain is fully filled with fluid under the conditions of non-isothermal, incompressible and non-slip of surfaces. At the same time, the inertia and gravitational forces are negligible. The form of the continuity and momentum equations are given as (Polyflow User's Guide, 2010)

$$\nabla \cdot \mathbf{v} = 0 \tag{1}$$
$$-\nabla P + \nabla \cdot \mathbf{\tau} = 0 \tag{2}$$

Where v is the velocity vector; *P is* the fluid pressure; t is stress tensor.
The stress tensor is described by

$$\mathbf{\tau} = 2\eta \, (\dot{\gamma}) \mathbf{D} \tag{3}$$

Where η is the shear viscosity, $\mathbf{D} = \frac{1}{2}\left[\nabla v + \left(\nabla v\right)^T\right]$ is the rate of deformation tensor, $\dot{\gamma}$ is the effective shear rate and given as

$$\dot{\gamma} = \sqrt{2\mathbf{D}:\mathbf{D}} \tag{4}$$

2.2 Materials

In this study, high-density polyethylene (PE) melt is used to the polymer processing in the tri-screw extruder. Due to the low shear rate in the experiment, it is appropriate to use the Carreau-Yasuda model to describe the rheological behavior of the blending as follows (Yasuda , 1981):

$$\eta = \eta_\infty + (\eta_0 - \eta_\infty)\left[1 + (\lambda\dot{\gamma})^a\right]^{\frac{n-1}{a}} \tag{5}$$

Where η_∞ is infinite shear viscosity, η_0 is the viscosity at zero shear viscosity, λ is a model-specific relaxation time and $\lambda = \sqrt{2\prod_{\mathbf{D}}}$, $II_{\mathbf{D}}$ is the second invariant of $\mathbf{D}$. n is the power-law index, which is a property of a given material. a represents the width of the transition region between η_0 and the power-law n. In this work, the parameters of the Carreau-Yasuda model for the PE melts at 463 K are described in Table 1(Bai *et al*., 2011).

Table 1 Parameters of the polyethylene with Carreau-Yasuda model

Param eters	ρ	η_0	η_∞	λ	n	a
PE	740 kg/m³	0 $Pa \cdot s$	1580 $Pa \cdot s$	0.17 s	0.70	0.64

2.3 Geometry and Meshing

The tri-screw extruder investigated in this work has three screws, which array in a triangle and are all co-rotation. In order to avoid screws interfering with one another, the numbers of screw flights are three, as shown in Fig.1. The stagger angle is an important factor to design and optimize the tri-screw extruder. Therefore, we focus on the effects of stagger angles on the flow and mixing efficiency in this work. The geometric models of the tri-screw extruder with three typical stagger angles, 30°, 60° and -30° corresponding to Tri-P30, Tri-N60 and Tri-R30 are depicted in Fig.2. The geometric parameters of three types of kneading disks for the tri-screw extruders are described in Table 2.

As illustrated in Fig.2, the Tri-P30 (pump element) has an ability to pump the fluid to the main transport direction due to the forward stagger angle. The Tri-R30 (reverse element) has a backward stagger angle and transports the material reverse to the main transport direction. The Tri-N60 is a neutral element and has not the ability to transport material backward or forward. The finite element (FE) models are established using Gambit software with the mesh superposition technique (MST) without re-meshing for the periodical geometric changes (Polyflow User's Guide, 2010). The

kneading elements and barrel are meshed individually. In order to catch the small velocity changes in the small clearances and near the walls, two boundary layer grids are employed in the FE model. At the same time, the refined grids are used in the special center region to catch the circumfluence phenomenon (Wang *et al.*, 2013).
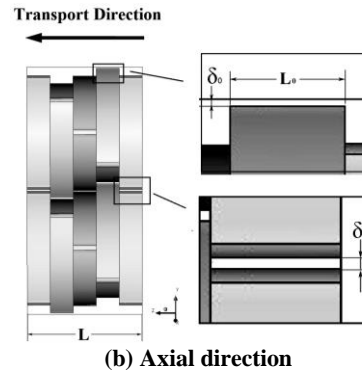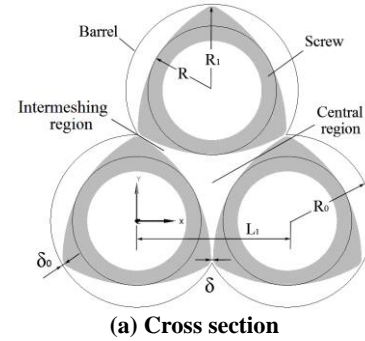

(a) Cross section

(b) Axial direction

Fig. 1. Geometric model of kneading disk for the tri-screw extruder.

Table 2 Geometrical configurations of the tri-screw extruder

Parameters	Symbols	Values
Screw root radius	R	13.0 mm
Screw tip radius	R_1	17.0 mm
Barrel radius	R_0	17.4 mm
Centerline of disk-disk	L_1	30.4mm
Depth of disk	L_0	6.0 mm
Total length	L	30.0 mm
Clearance of disk-disk	δ	0.4 mm
Clearance of disk-barrel	δ_o	0.4 mm
Disk flight numbers	n_1	3
Number of disks	n_2	5
	P30	$\alpha = 30°$
Stagger angles	N60	$\alpha = 60°$
	R30	$\alpha = -30°$

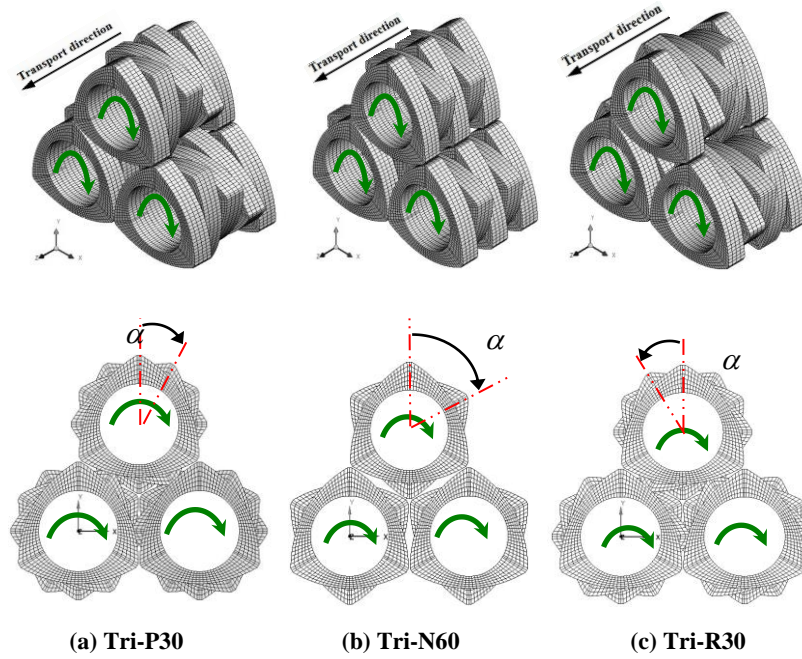**(a) Tri-P30**　　**(b) Tri-N60**　　**(c) Tri-R30**

Fig. 2. Meshes model with different staggering angle of kneading disks.

In order to make a comparison of the kneading disks between the tri-screw and twin-screw extruder, the geometrical parameters of the kneading disks for the twin-screw extruder are equal to the tri-screw extruder. The geometry models of the kneading disks with three typical stagger angles, 30, 60 and -30 degrees for the twin-screw extruder are defined as Twin-P30, Twin-N60 and Twin-R30, respectively, which are corresponding to the Tri-P30, Tri-N60 and Tri-R30 for the tri-screw extruders. It is noted that the mesh methods in the mixing section of the twin-screw extruder, such as element types, grid density, boundary layers and the MST are also the same as those of the tri-screw extruder.

During the numerical calculations, the mini-element and linear interpolations are used in the velocity and pressure calculations, respectively. The robust Picard iterative method is employed in the viscosity calculation due to the power-law index less than 0.75. The convergence accuracy level is 1×10^{-4} in all the simulations.

2.4 Evaluations of the mixing efficiency

Residence time distribution (RTD) function is an important parameter to determine the mixing performance of an extruder. The RTD density function, $E(t)$, shows the variation of the tracer concentration at the exit and is given by the following equation (Carneiro *et al.*, 2004):

$$E(t) = \frac{c(t)}{\int_0^t c(t)dt} = \frac{c(t)}{\sum_0^\infty c(t)\Delta t} \qquad (6)$$

Where $c(t)$ is the concentration of the trajectories at the exit. Δt is the time step. Another function related to $E(t)$ is accumulative residence time distribution function, $F(t)$, and given as:

$$F(t) = \int_0^t E(t)dt = \frac{\sum_0^t c(t)\Delta t}{\sum_0^\infty c(t)\Delta t} \qquad (7)$$

In order to accurately calculate the particle trajectories, a small iterative time step, $\Delta t = 0.025$s corresponding to 6° of screw rotation is employed. We have tested the accuracy with different numbers of particles setting freely on the inlet, such as 2000 particles and 3000 particles. It shows that the difference of their culmutive RTD with 2000 particles and 3000 particles is bellow 2%, which prove the accuracy.

In order to quantify and compare the RTD functions, we define three parameters, T_0, T_{75} and ΔT to characterize the RTD functions. T_0 means that the smallest time observed in the exit plane. T_{75} denotes time that 75% of the particles flow out of the exit. Whereas ΔT is equal to $T_{75} - T_0$.

In order to evaluate the dispersive mixing efficiency inside the screw extruders, the mixing index is employed and defined as (Cheng and Manas-Zloczower, 1990)

$$\lambda_{MZ} = \frac{|\mathbf{D}|}{|\mathbf{D}| + |\mathbf{W}|} \qquad (8)$$

Where W is the norm of the vorticity tensor. The fluid in screw extruder will be in the rotational and simple shear conditions with $\lambda_{MZ} = 0$ and $\lambda_{MZ} = 0.5$, respectively. Whereas the λ_{MZ} is 1.0 meaning the irrotational flow, such as pure elongational flow.

For the 3D flow in the tri-screw extruder, the local stretching of the material infinitesimal surface can be calculated from the mean value of the stretching η per calculated unit area. Then the area of stretch η can be expressed by (Manas-Zloczower, 1994)
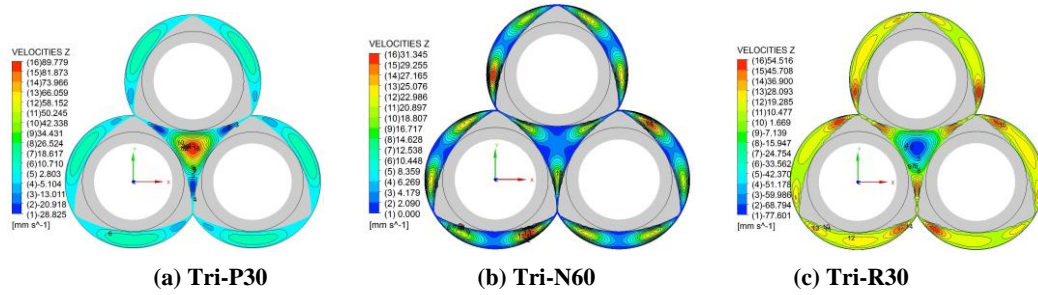
(a) Tri-P30　　　　**(b) Tri-N60**　　　　**(c) Tri-R30**

Fig. 3. Axial velocities in the kneading disks with maximal area of the center region.

(a) Tri-P30　　　　**(b) Tri-N60**　　　　**(c) Tri-R30**

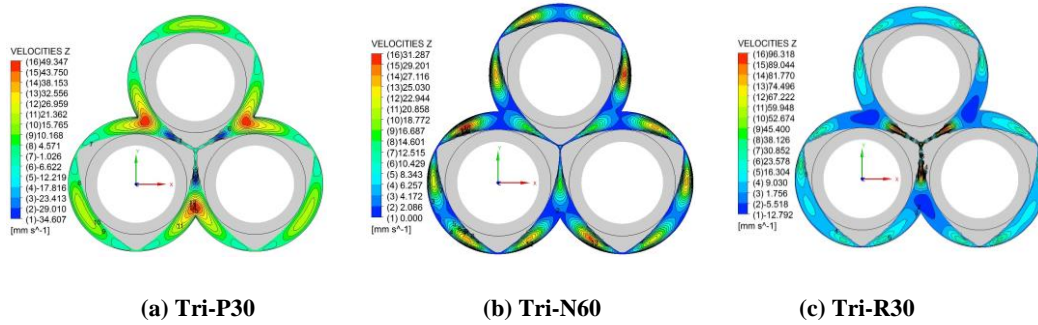**Fig. 4. Axial velocity distributions in the kneading disks with maximal area of the center region .**

$$\eta = \lim_{|dA| \to 0} \frac{|da|}{|d\mathbf{A}|} \qquad (9)$$

Where $d\mathbf{A}$ is an infinitesimal surface and deforms with time. The surface deformation at time dt is da .

3. RESULTS AND DISCUSSION

3 1 Effect of Stagger Angles on the Flow Patterns in Cross Sections

The tri-screw extruder, especially in the center region, has periodic geometrical configurations with screws rotation. In order to understand the effect of the center region area on the axial flow pattern in the kneading disks of tri-screw extruders with three typical stagger angles, the axial velocity (Z-velocity) profiles in the kneading disks with maximal and minimum areas of the center region are shown in Fig.3 and Fig.4, respectively.

Figure 3 shows the comparisons of axial velocity profiles in the cross-sections of the kneading disks with three stagger angles as the center regions of the tri-screw extruders have maximal areas. It can be seen from Fig. 3a that weak backflow (negative Z-velocity) in the intermeshing region between two screws and great axial velocity in the center region for the Tri-P30. However, there is no backflow pattern in the Tri-N60, as shown in Fig. 3b. In Fig.3c, the Z-velocity in the Tri-R30 is opposite to that in the Tri-P30, and the strong backflow exists in the middle of center region, where there are the great positive Z-velocities of polymer melt.

Figure 4 shows the Z-velocity profiles in the cross sections of the kneading disks with three kinds of

stagger angles, when the area of center regions of the tri-screw extruders is smallest. For the Tri-P30, it can be seen from Fig.4a that the backflow phenomenon appears in the screw tip region, and strong convey ability (great positive Z-velocity) presents in the joint region of screw channel between two screws. For the Tri-N60, there is strong positive Z-velocity at the screw tip region and no backflow phenomena, as shown in Fig.4b. And for the Tri-R30 in Fig.4c, we can see that great positive Z-velocity near the small center region and negative Z-velocity in the joint region of screw channels.

In comparison with Fig.3 and Fig.4, from the flow field of view, it is found that the axial velocities of materials in the center region of the Tri-P30 are faster than other kneading disks for tri-screw extruders. Therefore, the residence time in the center region of the Tri-P30 may be shorter than that of the Tri-N60 and Tri-R30. This is important to determine the homogeneity and quality of final products. The residence time of polymer melt in the Tri-R30 may be longest, though the Z-velocity is greatest when the area of center region is smallest. From the residence time point of view, the Tri-R60 may be best choice to gain homogeneous final products.

3. 2 Spatial Flow Law of Particles in Kneading Disks of Tri-Screw Extruders

Distributive mixing can be evaluated by particle tracking. In order to understand the special flow characteristics of the tri-screw extruder, the technology of particle tracking is used to follow the trajectories by using a fourth order explicit Runge-Kutta scheme. Initially, 2000 massless particles
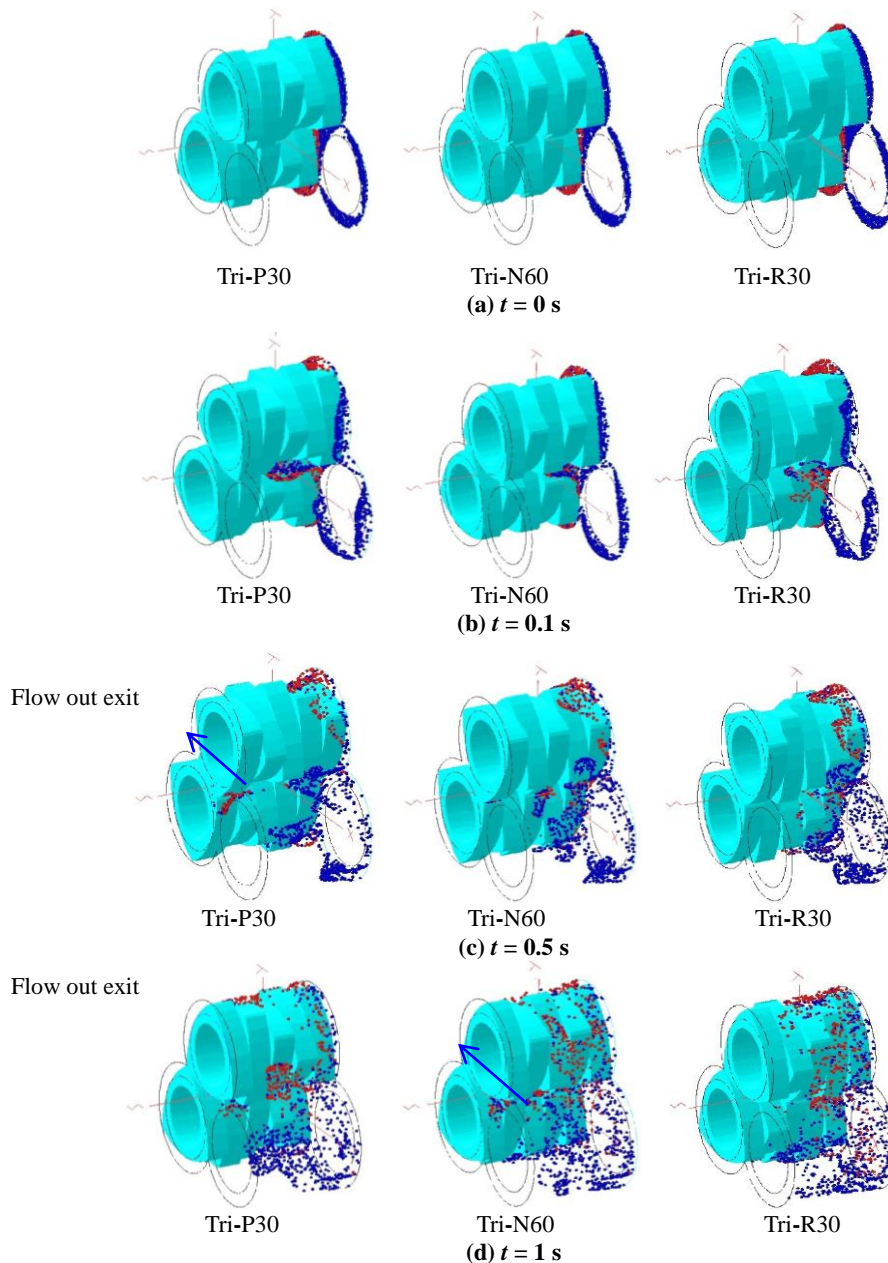
Tri-P30 Tri-N60 Tri-R30
(a) *t* **= 0 s**

Tri-P30 Tri-N60 Tri-R30
(b) *t* **= 0.1 s**

Flow out exit

Tri-P30 Tri-N60 Tri-R30
(c) *t* **= 0.5 s**

Flow out exit

Tri-P30 Tri-N60 Tri-R30
(d) *t* **= 1 s**
Fig. 5. Flow processes of polymer particles in the mixing sections of tri-screw extruders.

with two kinds of colors are set freely throughout the inlet section (see Fig.5a). The transient motions of particle tracking in tri-screw extruder with a rotational speed of 40 rpm are described in Fig.5. From Fig.5b and Fig.5c, it is found that most of particles initially in the center region of the Tri-P30 quickly move in the center region along axial distance due to the great axial velocities. This is similar to the convey element of the tri-screw extruder (Yoshinaga *et al.*, 2000). The particles in the Tri-P30 begin to flow out the exit at 5 s, as shown in Fig.5c, and in the Tri-N60 at 1.0 s, as shown in Fig.5d. However, with the increase in stagger angles, above phenomenon takes off gradually in the Tri-N60 and Tri-R30. With the increase of mixing time, the particles diffuse into the whole flow region of the kneading disks, as shown in Fig.5d. In comparison with three kinds of

kneading disks, it is found that the Tri-R30 has more even distribution of particles than the Tri-P30 and Tri-N60. This implies that the Tri-R30 has relatively better distributive mixing efficiency.

3.3 Dispersive Mixing Efficiency

The purpose of mixing is to break up and extend the dispersed phase in continuous phase. The shear rate and maximum stress magnitudes are important parameters to evaluate the dispersive mixing for the mixers. Figure 6 shows the mean shear rates along the axial length between the tri-screw and twin-screw extruders. It is found that the mean shear rates of polymer melts increase in the kneading disk edges and decrease in the kneading disk channel within the twin-screw and tri-screw extruders. In comparison with the twin-screw and tri-screw

extruders, we can observe that the values of mean shear rates in mixing section of the tri-screw extruder are bigger than those of the twin-screw extruder at the same stagger angles. This reveals that the kneading disks of tri-screw extruder have greater dispersive mixing efficiency than those of twin-screw extruder. Meanwhile, the Tri-R30 has biggest value of the mean shear rate followed by the Tri-N60, and the Tri-P30 has minimal value of the mean shear rate.
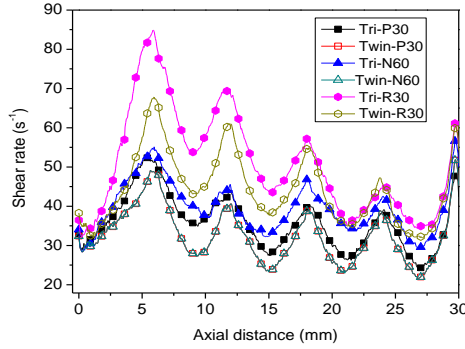

Fig. 6. Comparisons of mean shear rates along the axial length between the tri-screw and twin-screw extruders.

Figure 7 shows the comparisons of maximal stress magnitudes along the axial length of the screws between the tri-screw and twin-screw extruders. It is found that increasing the axial distance increases the maximal stress magnitudes in the screw extruders. Moreover, with the increase of stagger angles, the maximal stress magnitudes within the twin-screw and tri-screw extruders increase. By comparison, it is found that the kneading disks of tri-screw extruder have greater maximal stress magnitude than those of twin-screw extruder with the same stagger angles, indicating the better dispersive mixing efficiency induced by stress in the tri-screw extruder.
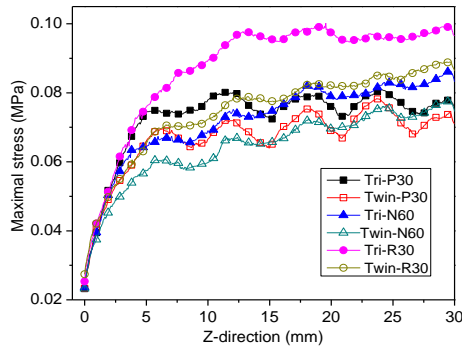

Fig. 7. Comparisons of maximal stress along the axial length between the tri-screw and twin-screw extruders.

The shear rate and comparison the percentage of the material particles with a certain value of shear rate within three typical kneading disks of the tri-screw extruders are illustrated in Table 3. The probabilities with the shear rates larger than 50 s^{-1} in the Tri-P30, Tri-N60 and Tri-R30 are 8.14%, 13.68% and 27.95%, respectively. The probabilities with the shear rates larger than 100 s^{-1} in the Tri-

P30, Tri-N60 and Tri-R30 are 7.75%, 8.58% and 7.89%, respectively. And the probabilities with the values of shear rates greater than 200 s^{-1} in the Tri-P30, Tri-N60 and Tri-R30 are 7.76%, 8.56% and 7.13%, respectively. The results in Table 3 show that the material particles in the Tri-N60 and Tri-R30 have higher probability to obtain higher shear rate than in the Tri-P30. Thus, the neutral and reverse kneading disks, Tri-N60 and Tri-R30, have predicted better mixing abilities for the mixing sections of tri-screw extruders.

Table 3 Characteristic values for three typical stagger angles of knead disks in tri-screw extruders at speed of 40 rpm

Property	Element		
	Tri-P30	Tri-N60	Tri-R30
Pressure drop (MPa)	0.03	-0.556	-1.165
particles with shear rate (s^{-1})			
>50%	8.14	32.465	27.95
>100%	7.75	8.4241	7.89
>200%	7.76	6.817	7.13

Mixing index is an important parameter to evaluate the dispersive mixing in the extruders. The comparisons of mixing index along the axial length between the tri-screw and twin-screw extruders are shown in Fig.8. It can be seen that the kneading disk of tri-screw extruder has greater mixing index magnitude than that of twin-screw extruder at the same stagger angles. It reveals that the tri-screw extruder has greater dispersive mixing efficiency than the twin-screw extruder for the mixing sections. By comparison the twin-screw and tri-screw extruders, it can be observed that the difference of mixing index value between the Tri-N60 and Twin-N60 is bigger than that between Tri-R30 and Twin-R30. This may be due to the fact that the Tri-N60 has greater axial velocities in the center region than the Tri-R30. In addition, the mixing index distribution in the Tri-P30 is similar to in the Twin-P30 due to the great axial velocities of material in the center region of the Tri-P30.
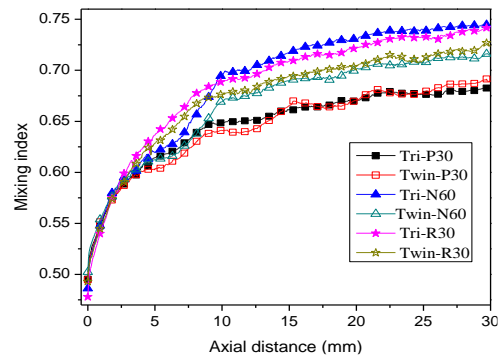

Fig. 8. Comparisons of mixing index along the axial length between the tri-screw and twin-screw extruders.

It is well known that the stretch flow is more effective than shear flow on mixing efficiency in polymer process (Ottino et al., 1981）. The probabilities of maximal stretching rate is the number of the particles that go through maximal stretching rate at mixing time, respectively. Figure 9 shows the comparisons of probability of maximal stretching rate between tri-screw and twin-screw extruders with different stagger angles. The probability curves of maximum stretching rate in the mixing sections of the tri-screw extruders locate on right of the twin-screw extruders. This illuminates that the mixing sections of the tri-screw extruders have a higher probability to gain the elongational flow than those of the twin-screw extruders at the same stagger angles. Furthermore, it can be observed from Fig.9 that the probabilities with the maximal stretching rate larger than 80 s^{-1} are 14%, 10% and 22% in the Tri-P30, Tri-N60 and Tri-R30, respectively. Therefore, the Tri-R30 has better stretching rates than other kneading disks for the tri-screw extruders.
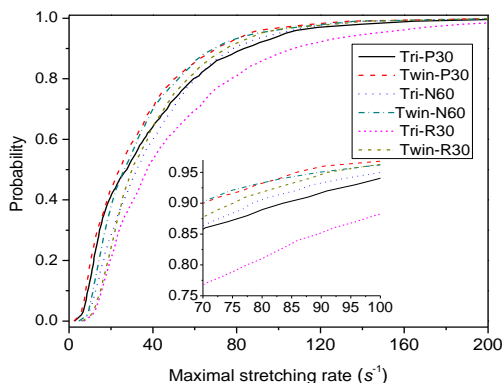

Fig. 9. Comparisons of probability of maximal stretching rate between tri-screw and twin-screw extruders with different stagger angles.

3.4 Residence Time Distribution

Distributive mixing performance in mixers can be evaluated by the residence time distribution (RTD). Based on the velocity profiles and particle trajectories, the cumulative RTD distributions in the kneading disks of the tri-screw and twin-screw extruders are calculated, as shown in Fig. 10. It can be seen that the cumulative RTD curve in the Tri-P30 has an obvious flat section, which is different from the conventional single-screw and twin-screw extruders. The T0 of the Tri-P30 is shorter than the Tri-N60 and Tri-R30, which is disadvantageous for the homogeneity of the final products. This is due to the fact that the Tri-P30 has great axial velocity of polymer melt in the center region (see Fig.3a). At the same time, the pressure differences between inlet and outlet for three kinds of kneading disks are extremely significant, as shown in Table 3. The pressure difference between the inlet and outlet in the Tri-P30 increases to 0.03 MPa due to its strong pump ability with forward stagger angle. Also, it is contributed to decrease the minimum residence time. The pressure difference in the Tri-R30 decreases 1.165 MPa due to the reverse of the main

transport direction. This decreasing pressure difference is benefit to increase the minimum residence time. Whereas the pressure difference in the Tri-N60 decreases 0.505 MPa. Therefore, from the pressure difference of view, the minimum residence time in the Tri-P30 is shorter than that in the Tri-N60 and Tri-R30.
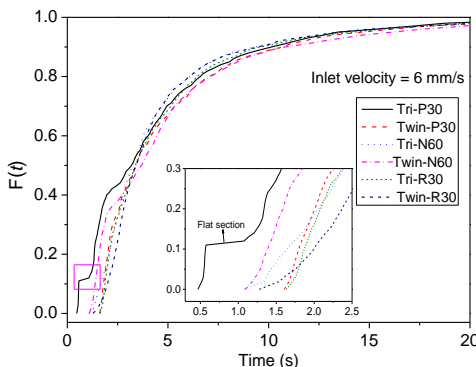

Fig. 10. Cumulative RTD in the kneading disks of tri-screw and twin-screw extruders

The RTD profiles and information of the T_0, T_{75} and ΔT in the Tri-P30, Tri-N60 and Tri-R30 are compared with in Twin-P30, Twin-N60 and Twin-R30 at speed of 40 rpm are depicted in Fig.11 and Table 4, respectively. It is well known that the minimal residence time is an important parameter to determine the homogeneity of the final products. From Table 4, the minimal residence time in the Tri-P30 is 0.47 s (This also can be observed in Fig.5c), and much smaller than those in Tri-N60 and Tri-R30. The trends of kneading disks of twin-screw extruders are similar to that of tri-screw extruders, but the value of the RTD in the Twin-P30 is bigger than that in the Tri-P30. On the other hand, the large distribution of the residence time is the sign of inhomogeneities and is disadvantageous to acquire good final products. Out of question, it is ideal that all the particles flow out the exit with same residence time. Therefore, it can be concluded that the RTD distribution in the Tri-R30 is relatively reasonable for the tri-screw extruder. However, the RTD distribution of the Twin-N60 is relatively reasonable for the twin-screw extruder. These differences in the mixing section between of the twin-screw and tri-screw extruders are mainly due to great axial velocities of polymer melt in the center region.
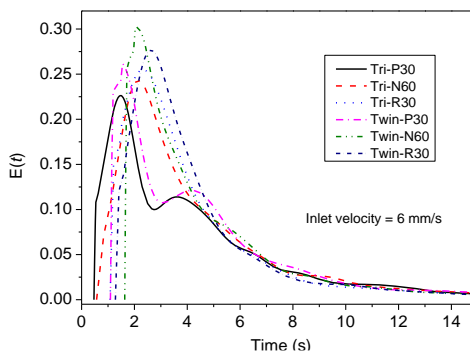

Fig. 11. RTD profiles in the mixing sections of the tri-screw and twin-screw extruders.

Table 4 Effects of stagger angles on the RTD in the knead disks at speed of 40 rpm

RTD	T_0	T_{75}	$\Delta T = T_{75} - T_0$
Tri-P30	0.47	7.71	7.24
Tri-N60	0.56	5.91	5.35
Tri-R30	1.08	5.54	4.46
Twin-P30	1.09	6.67	5.58
Twin-N60	1.63	5.88	4.25
Twin-R30	1.27	5.29	4.02

3.5 Logarithm of Area Stretch

The mean logarithm of the area stretch usually is used to measure the dispersive mixing ability for a mixer. The calculated mean logarithm of the area stretch for the different screw extruders at different stagger angles is described in Fig.12. It can be seen that with the increase of mixing time, all the logarithm of the area stretch increases exponentially in the twin screw and tri-screw extruder, which is of benefit to efficient laminar mixing. In comparison with the mixing sections of tri-screw and twin-screw extruders at same stagger angles, it is obvious that the values of the logarithm of area stretch in the tri-screw extruder are much larger than those in twin screw extruder due to the great folding and stretch of materials in the tri-screw extruder. Moreover, the results in Fig.12 show that the Tri-R30 has higher stretching efficiency than other kneading disk configures, indicating the better distributive mixing.

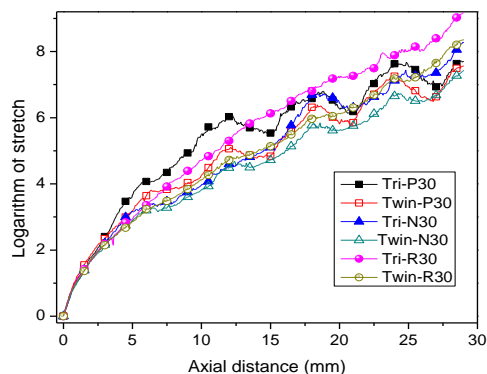**Fig. 12. Logarithm of the area stretch in the kneading disks of tri-screw and twin-screw extruders with different stagger angles.**

4. CONCLUSION

In this paper, three-dimensional finite element modeling of polymer melt flow and mixing in the kneading disks of a novel tri-screw extruder was established. The flow visualizations in the kneading disks of tri-screw extruders were carried out with particle trajectories. Moreover, the dispersive and distributive mixing efficiencies in the kneading disks of the tri-screw and the twin-screw extruders were compared.

The results show that, firstly, the kneading disks in the tri-screw extruder have greater shear rate, stretching rates, maximal stress magnitudes and mixing index than in the twin-screw extruder with

same stagger angles. Therefore, the mixing sections of the tri-screw extruder have greater distributive mixing efficiencies than those of the twin-screw extruder. Meanwhile, the Tri-R30 has highest distributive mixing efficiency than other kneading disks in the tri-screw extruder, followed by Tri-N60 and Tri-P30. On the other hand, the pump element of kneading disk, Tri-P30, has great axial velocities of polymer melt in the center region, which is similar to the convey element of the tri-screw extruder. However, increasing the stagger angles decreases the axial velocities of polymer melt in the center region, such as for the Tri-N60 and Tri-R30. This phenomenon induces the difference in the RTD characteristics of the kneading disks between the twin-screw and tri-screw extruders. In RTD, the Tri-R30 is relatively reasonable for the tri-screw extruder, and the Twin-N60 is relatively reasonable for the twin-screw extruder. Finally, the logarithm of the area stretch in the tri-screw extruder is much larger than in the twin screw extruder due to the great folding and stretch material in the tri-screw extruder. Moreover, the Tri-R30 has higher stretching efficiency than other kneading disk configures in the tri-screw extruder. So the Tri-R30 has higher dispersive mixing efficiency than other kneading disk configures.

REFERENCES

Alsteens, B., V. Legat and T. Avalosse (2004). Parametric study of the mixing efficiency in a kneading block section of a twin-screw extruder. *International Polymer Processing* 19(3), 207-217.

ANSYS Inc. Polyflow User's Guide (2010). Release 13.0 of ANSYS Inc.

Bai, Y., U. Sundararaj and K. Nandakumar (2011). Nonisothermal modeling of heat transfer inside an internal batch mixer. *AIChE Journal*, 57(10), 2657-2669.

Bravo, L. V., A. N. Hrymak and J. D. Wricht (2004). Study of particle trajectories, residence times and flow behavior in kneading discs of intermeshing co-rotating twin-screw extruders. *Polymer Engineering and Science* 44(4),779-793.

Carneiro, O. S., J. A. Covasa and J. A. Ferreira (2004). On-line monitoring of the residence time distribution along a kneading block of a twin-screw extruder. *Polymer testing,* 23(8),925–937.

Cheng, J. J. and I. Manas-Zloczower (1990). Flow

field characterization in a banbury mixer. *International Polymer Processing* V(3), 78–183.

Ghoreishy, M. H. R. and G. Naderi (2005) Three-dimensional finite element modeling of rubber curing process. *Journal of Elastomers and Plastics* 37(1), 37-53.

Huang, C. K. and F. S. Cheng (2009). Study on Kneading and Molding of PP/TiO$_2$ Nanocomposite. *International Polymer Processing* 24(3), 267-271.

Hu, D. and J. Chen (2004). Simulation of 3D isothermal flow in intermeshing co-rotating tri-screw extruders. *Journal of Chemical Industry and Engineering* 55(2), 280–283.

Hu, D. and J. Chen (2006). Simulation of polymer melts flow fields in intermeshing co-rotating three-screw extruders. *Journal of Beijing Institute of Technology* 15(3), 360-365.

Ishikawa, T., S. Kihara and K. Funatsu (2001). 3-D non-isothermal flow field analysis and mixing performance evaluation of kneading blocks in a co-rotating twin screw extruder. *Polymer Engineering and Science* 41(5), 840–849.

Jiang, N. and C. W. Zhu (2001). Analysis of mixing performance in a triple screw extruder. *China Plastic* 15, 87–91.

Jiang, N. and C. W. Zhu (2008). Study on extrusion characteristics of the tri-screw extruder. *Polymer-Plastics Technology and Engineering* 47(6), 590-594.

Li W. G (2011). Blade exit angle effects on performance of a standard industrial centrifugal oil pump. *Journal of Applied Fluid Mechanics* 4(2), 105-119.

Manas-Zloczower, I. (1994). Studies of mixing efficiency in batch and continuous mixers. *Rubber Chemistry and Technology* 67(3),504–528.

Nakayama, Y., E.Takeda and T. Shigeishi (2011). Melt-mixing by novel pitched-tip kneading disks in a co-rotating twin-screw extruder. *Chemical Engineering Science* 66(1),103–110.

Nili-Ahmadabadi M., M. Durali and A. Hajilouy (2014). A novel aerodynamic design method for

centrifugal compressor impeller. *Journal of Applied Fluid Mechanics* 7(2), 329-344.

Ottino, J. M., C. W. Macosko and W. E. Ranz (1981). A Framework for the description of mechanical mixing of fluids. *AIChE Journal* 27, 565-577.

Rafei, M., M. H. R. Ghoreishy and G. Naderi (2009). Development of an advanced computer simulation technique for the modeling of rubber curing process. *Computational Materials Science* 47(2), 539-547.

Sobhani, H., M. Razavi-Nouri and M. H. R. Ghoreishy (2010). Quasi-steady state finite element modelling of polymer melt flow in an intermeshing co-rotating twin screw extruder. *Iranian Polymer Journal* 19(2), 143-154.

Wang, G., X. Z. Zhu and Y. D. He (2013). Effects of Screw Clearance and Blend Ratio on the Flow and Mixing Characteristics of Tri-Screw Extruders in the Cross Section with CFD. *Engineering Applications of Computational Fluid Mechanics* 7(1),74-89.

Yasuda, K., R. C. Armstrong and R. E. Cohen (1981). Shear low properties of concentrated solutions of linear and star branched polystyrenes. *Rheological Acta* 20(2), 163-178.

Yoshinaga, M., M. Miyazaki and L. J. Liu (2000). Mixing Mechanism of Three-tip Kneading Block in Twin Screw. Extruders. *Polymer Engineering and Science* 40(1),168–178.

Zhu, X. Z., Y. J. Xie and Y. Miao (2009). Numerical study on temperature and power consumption of intermeshing co-rotation triangle arrayed tri-screw extruders. *Polymer-Plastics Technology and Engineering* 48(4), 367-373.

Zhu, X. Z., G. Wang and Y. D. He (2013 b) Study on dynamic flow and mixing Performances of tri-screw extruders with finite element method. *Advances in Mechanical Engineering*, Article 1-12.

Zhang, X. M., L. F. Feng and W. X. Chen (2009). Numerical simulation and experimental validation of mixing performance of kneading discs in a twin screw extruder. *Polymer Engineering and Science* 49(9),1772-1783.